Brain, Behavior, and Immunity 123 (2025) 1011–1023

Contents lists available at ScienceDirect

Brain Behavior and Immunity

journal homepage: www.elsevier.com/locate/ybrbi

Acute exercise boosts NAD^+ metabolism of human peripheral blood mononuclear cells

David Walzik [a], Niklas Joisten [a,b], Alexander Schenk [a], Sina Trebing [a], Kirill Schaaf [c], Alan J Metcalfe [d], Polyxeni Spiliopoulou [e], Johanna Hiefner [f], Adrian McCann [g], Carsten Watzl [h], Per Magne Ueland [g], Sebastian Gehlert [i], Anna Worthmann [f], Charles Brenner [j], Philipp Zimmer [a,*]

[a] Department of Performance and Health (Sports Medicine), Institute for Sport and Sport Science, TU Dortmund University, Otto-Hahn-Straße 3, 44227 Dortmund, Germany
[b] Division of Exercise and Movement Science, Institute for Sport Science, University of Göttingen, Sprangerweg 2, 37075 Göttingen, Lower Saxony, Germany
[c] Department of Molecular and Cellular Sports Medicine, Institute of Cardiovascular Research and Sports Medicine, German Sport University Cologne, Am Sportpark Müngersdorf 6, 50933 Cologne, Germany
[d] Chest Unit, Centre for Human and Applied Physiological Sciences (CHAPS), Denmark Hill Campus, King's College Hospital, King's College London, London, United Kingdom
[e] Sports Performance Laboratory, School of Physical Education and Sport Science, National and Kapodistrian University of Athens, 172 37 Athens, Greece
[f] Department of Biochemistry and Molecular Cell Biology, University Medical Center Hamburg-Eppendorf, Martinistraße 52, 20246 Hamburg, Germany
[g] Bevital AS, Frydenbøgården 5. etg., Minde Allé 35, 5068 Bergen, Norway
[h] Leibniz Research Center for Working Environment and Human Factors at TU Dortmund (IfADo), Ardeystraße 67, 44139 Dortmund, Germany
[i] Department for the Biosciences of Sports, Institute of Sports Science, University of Hildesheim, Universitätsplatz 1, 31141 Hildesheim, Germany
[j] Department of Diabetes and Cancer Metabolism, Beckman Research Institute, City of Hope National Medical Center, 1500 East Duarte Road, Duarte, CA 91010, USA

ARTICLE INFO

Keywords:
Exercise
Immune cell
Metabolism
Nicotinamide adenine dinucleotide
NAD^+
PBMC

ABSTRACT

Nicotinamide adenine dinucleotide (NAD^+) coenzymes are the central electron carriers in biological energy metabolism. Low NAD^+ levels are proposed as a hallmark of ageing and several diseases, which has given rise to therapeutic strategies that aim to tackle these conditions by boosting NAD^+ levels. As a lifestyle factor with preventive and therapeutic effects, exercise increases NAD^+ levels across various tissues, but so far human trials are mostly focused on skeletal muscle. Given that immune cells are mobilized and redistributed in response to acute exercise, we conducted two complementary trials to test the hypothesis that a single exercise session alters NAD^+ metabolism of peripheral blood mononuclear cells (PBMCs). In a randomized crossover trial (DRKS00017686) with 24 young adults (12 female) we show that acute exercise increases gene expression and protein abundance of several key NAD^+ metabolism enzymes with high conformity between high-intensity interval training (HIIT) and moderate-intensity continuous training (MICT). In a longitudinal exercise trial (DRKS00029105) with 12 young adults (6 female) we confirm these results and reveal that – similar to skeletal muscle – NAD^+ salvage is pivotal for PBMCs in response to exercise. Nicotinamide phosphoribosyltransferase (NAMPT), the rate-limiting enzyme of NAD^+ salvage pathway, displayed a pronounced increase in gene expression during exercise, which was accompanied by elevated intracellular NAD^+ levels and reduced serum levels of the NAD^+ precursor nicotinamide. These results demonstrate that acute exercise triggers NAD^+ biosynthesis of human PBMCs with potential implications for immunometabolism, immune effector function, and immunological exercise adaptions.

* Corresponding author.
E-mail address: philipp.zimmer@tu-dortmund.de (P. Zimmer).

https://doi.org/10.1016/j.bbi.2024.11.004
Received 24 July 2024; Received in revised form 27 October 2024; Accepted 2 November 2024
Available online 3 November 2024

1. Introduction

Under physiological conditions, NAD^+ levels are maintained via four distinct routes: (1) *de novo* synthesis from the essential amino acid tryptophan along the kynurenine pathway, (2) incorporation of nicotinic acid and trigonelline (Membrez et al., 2024) into the Preiss-Handler pathway, (3) intracellular recycling of NAD^+ via nicotinamide salvage, and (4) salvage of nicotinamide riboside (Fig. 1) (Trammell et al., 2016). While tryptophan, nicotinic acid, trigonelline, and nicotinamide riboside require transmembrane transporters for cellular uptake, nicotinamide crosses cell membranes via simple diffusion. Cellular routes of NAD^+ biosynthesis also differ in terms of enzymatic reactions needed to yield NAD^+. For instance, nicotinamide salvage is achieved via two enzymatic reactions involving NAMPT and nicotinamide nucleotide adenylyltransferases (NMNAT1-3). Similarly, nicotinamide riboside requires nicotinamide riboside kinases (NRK1-2) (Bieganowski and Brenner, 2004), and NMNAT1-3 to yield NAD^+ (Fig. 1). In contrast, *de novo* synthesis via the kynurenine pathway requires eight enzymatic reactions and one spontaneous cyclization with metabolic intermediates along this pathway also serving as precursors for other end products such as kynurenic acid or acetyl coenzyme A (Schwarcz et al., 2012). Ultimately, the tissue-specific bioavailability of NAD^+ precursors and the enzymatic makeup of different target cells dictates the metabolic flux along each of these biosynthesis pathways with considerable variation between species, tissues, and cell types (Liu et al., 2018; Bogan and Brenner, 2008; Palzer et al., 2018).

Alterations in cellular NAD^+ homeostasis are a common feature of numerous conditions of metabolic stress (Katsyuba et al., 2020; Zapata-Pérez et al., 2021), including DNA damage (Fang et al., 2016), central (Vaur et al., 2017) and peripheral neurodegeneration (Di Stefano et al., 2015), heart failure (Diguet et al., 2018), fatty liver disease (Trammell et al., 2016), and viral infection (Heer et al., 2020). Additionally, tissue-specific NAD^+ levels are decreased in several rodent models of ageing (Yoshino et al., 2018), and initial evidence suggests that this also applies to humans (Covarrubias et al., 2021; Peluso et al., 2021). Restoring cellular NAD^+ levels is thus considered a promising therapeutic approach, and different NAD^+-boosting strategies have shown positive results in animal disease models (Yoshino et al., 2018) and clinical populations (Rajman et al., 2018). For instance, oral supplementation with the NAD^+ precursor nicotinamide riboside increases NAD^+ levels in human PBMCs (Trammell et al., 2016; Martens et al., 2018) and brain tissue of Parkinson's disease patients (Brakedal et al., 2022). Similarly, supplementation with the NAD^+ precursor nicotinamide mononucleotide stimulated mitophagy and reversed memory impairments in animal models of Alzheimer's disease (Fang, 2019; Fang et al., 2019). Tissue-specific NAD^+ levels are also boosted by acute exercise and exercise training (Walzik et al., 2023), although human trials are so far mostly focused on skeletal muscle (Chubanava and Treebak, 2023; Costford et al., 2010; de Guia et al., 2019). Given that the onset of acute exercise is characterized by a myriad of physiological alterations that reach far beyond skeletal muscle itself, other tissues might also display increased NAD^+ levels due to the higher metabolic activity resulting from sympathetic activation. Specifically, acute exercise mobilizes and redistributes immune cells (Schlagheck et al., 2020), and this exercise-induced relocation is considered a preventive and therapeutic mechanism in medical conditions like cardiovascular disease (Janssen et al., 2023), infections (Campbell and Turner, 2018), and cancer (Campbell et al., 2024; Fiuza-Luces et al., 2024). While the physiological basis of these immune effects is well established, the immunometabolic underpinnings remain poorly characterized. Previous investigations have successfully linked intracellular NAD^+ levels to immune effector functions such as viral defense (Holay et al., 2023) or cellular cytotoxicity against tumors (Guo et al., 2023; Wang et al., 2021; Wan et al., 2023). Additionally, several clinical trials have demonstrated that nicotinamide riboside supplementation mediates anti-inflammatory effects such as lower proinflammatory cytokine expression in PBMCs of heart failure

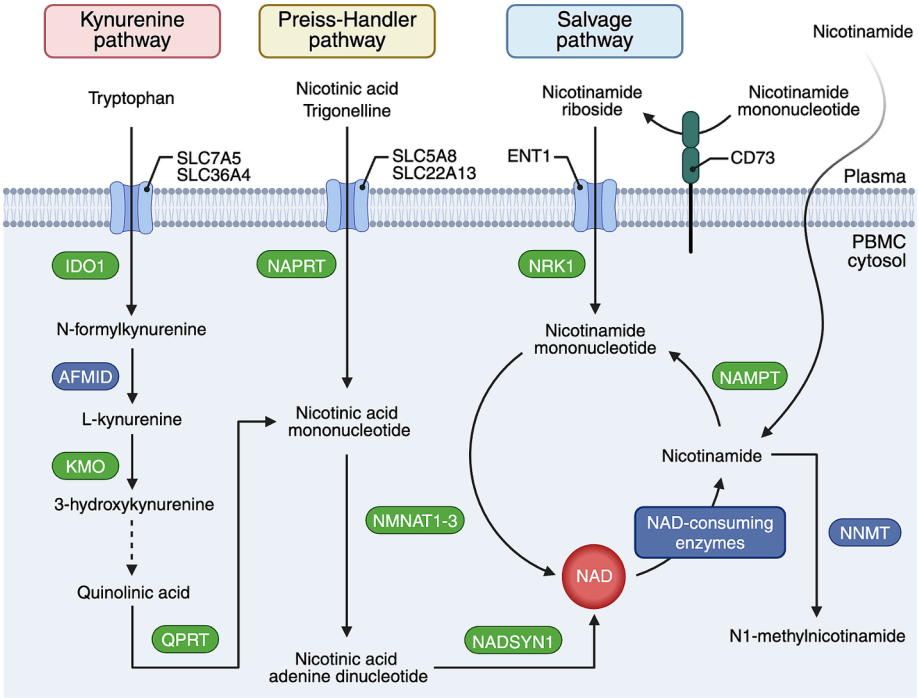

Fig. 1. Overview of cellular NAD^+ metabolism. Intracellular NAD^+ levels are maintained via the kynurenine pathway, the Preiss-Handler pathway, and a salvage pathway. Key enzymes selected for analysis of gene expression and protein abundance in this work are highlighted in green. Figure adapted from ref. Covarrubias et al. (2021). AFMID, arylformamidase; CD, cluster of differentiation; ENT1, equilibrative nucleoside transport 1; IDO1, indoleamine 2,3-dioxygenase 1; KMO, kynurenine 3-monooxygenase; NAD^+, nicotinamide adenine dinucleotide; NADSYN1, NAD synthetase 1; NAMPT, nicotinamide phosphoribosyltransferase; NAPRT, nicotinate phosphoribosyltransferase; NMNAT1-3, nicotinamide nucleotide adenylyltransferase 1-3; NRK1, nicotinamide riboside kinase 1; NNMT, nicotinamide N1-methyltransferase; QPRT, quinolinate phosphoribosyltransferase; SLC, solute carrier. Created with BioRender.com

patients (Wang et al., 2022; Zhou et al., 2020), blunted IFN-ɣ and IL-17 secretion in CD4$^+$ T cells of psoriasis patients (Han et al., 2023), and reduced autophagy and IFN-β secretion in monocytes of systemic lupus erythematosus patients (Wu et al., 2022). This suggests that supplementation with nicotinamide riboside boosts NAD$^+$ metabolism and effector function of immune cells. Whether exercise, a further NAD$^+$-boosting strategy (Walzik et al., 2023), exerts similar effects on immune cells, however, remains unclear to date.

Here, using two complementary trials, we test the hypothesis that acute exercise boosts NAD$^+$ metabolism of PBMCs. In a randomized crossover trial, we investigate the impact of exercise intensity and sex on gene expression and protein abundance of key NAD$^+$ metabolism enzymes of PBMCs (Fig. 2a). In a subsequent longitudinal trial, we make use of high temporal resolution to characterize the gene expression kinetics of NAD$^+$ metabolism enzymes during acute exercise and assess the impact of exercise on serum precursors and intracellular metabolites of NAD$^+$ metabolism (Fig. 2b).

2. Results

2.1. Impact of exercise intensity and sex on NAD$^+$ metabolism of PBMCs (trial 1)

Preclinical research suggests that exercise increases macrophage IDO1 activity with potential implications for *de novo* NAD$^+$ biosynthesis (Ito et al., 2003). We have recently reported that a single exercise session increases gene expression of kynurenine pathway enzymes in human PBMCs (Joisten et al., 2024), but it remains unclear whether this facilitates NAD$^+$ production. To investigate the impact of exercise on NAD$^+$ metabolism of PBMCs, we analyzed gene expression of key NAD$^+$ metabolism enzymes before, immediately after, and 1 h after exercise (see enzymes highlighted in green in Fig. 1). We recruited 24 healthy recreational runners (12 female) for a randomized crossover trial comparing two established exercise paradigms: high-intensity interval training (HIIT) and moderate-intensity continuous training (MICT, for in- and exclusion criteria see Supplementary Table S1). To compare exercise intensity-dependent differences between HIIT and MICT, we designed the exercise sessions in a time- and energy-matched fashion (for details see Methods). Participants exhibited a mean VO_{2peak} of 56.64 ± 6.43 ml min^{-1} kg^{-1}, corresponding to the top 10th percentile compared to age- and sex-matched reference values (Kaminsky et al.,

Table 1
Participant characteristics of trial 1 separated by exercise sequence.

	HIIT − MICT (N = 10)			MICT − HIIT (N = 14)			Group differences
	Min	Max	Mean ± SD	Min	Max	Mean ± SD	P value
Sex [m/f]	NA	NA	5/5	NA	NA	7/7	NA
Age [years]	22	35	30 ± 3.94	21	35	29.43 ± 4.72	0.758
Height [cm]	168	184	175.6 ± 6.43	164	192	177.93 ± 9.47	0.508
Weight [kg]	59.4	80.2	68.83 ± 7.51	50.5	94.4	70.33 ± 13.45	0.754
BMI [kg m^{-2}]	20.3	24.5	22.16 ± 1.3	17.4	27.2	22.34 ± 2.98	0.941
RPE_{max} [A.U.]	18	20	19.7 ± 0.68	17	20	19.14 ± 1.17	0.19
VO_{2peak} [mL kg^{-1} min^{-1}]	47.6	66.9	56.75 ± 7.08	49.5	68.9	56.56 ± 6.19	0.944
HR_{max} [min^{-1}]	153	193	177 ± 13.07	168	201	184.85 ± 8.7	0.0986

Two-sided, unpaired, *t*-tests were performed to assess group differences between the two exercise sequences HIIT-MICT and MICT-HIIT.

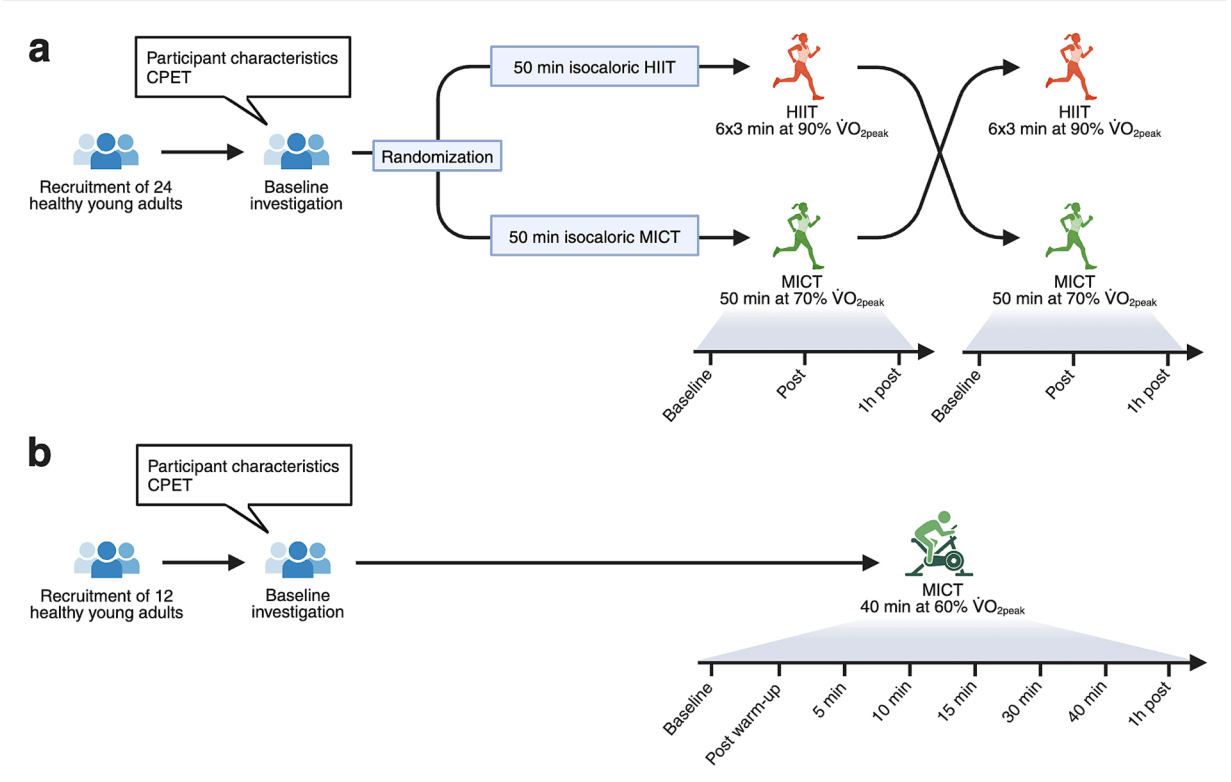

Fig. 2. Study outline. (a) Study design of the randomized crossover trial. (b) Study design of the longitudinal exercise trial. For details on the participant flow of both trials see Fig. S1 and S2. CPET, cardiopulmonary exercise test; HIIT, high-intensity interval training; MICT moderate-intensity continuous training; VO_{2peak}, peak oxygen uptake. Created with BioRender.com.

2022). Participant characteristics did not differ between the two exercise sequences (HIIT-MICT, MICT-HIIT), indicating that our randomization was unbiased (Table 1). To quantify the interindividual variation of the outcomes assessed in this trial we calculated coefficients of variation (CVs). The overall mean CV for all outcomes was 23.95 % (Fig. S3a), which is similar to what was previously reported in a human exercise trial (Savikj et al., 2022). Detailed CVs for all outcomes separated by exercise condition and measurement timepoint are displayed in Fig. S3a-c. Aiming to identify both, intensity-dependent and sex-dependent differences in gene expression of PBMCs, we made use of linear mixed models with exercise condition (HIIT, MICT), sex (male, female), and time (baseline, post exercise, 1 h post exercise) as fixed effects and participant ID as random effect (see Supplementary Table S2). These linear mixed models were followed by analyses of variance (ANOVA) and pairwise comparisons in case of significant results.

2.1.1. Gene expression of salvage pathway enzymes is dependent on exercise intensity

Interestingly, significant time condition interaction effects were only found for NAD^+ salvage pathway enzymes *NMNAT1* ($F_{2,96.79} = 4.72$, $P_{ANOVA} = 0.011$) and *NAMPT* ($F_{2,99.48} = 4.18$, $P_{ANOVA} = 0.018$). Detailed ANOVA results of all analyzed genes are displayed in Supplementary Table S3. Pairwise comparisons revealed higher gene expression of *NAMPT* immediately after MICT compared to HIIT ($P = 0.0062$). In contrast, 1 h after exercise, gene expression of *NMNAT1* was higher in HIIT compared to MICT ($P = 0.0017$; Fig. 3a). These results indicate that PBMC gene expression of NAD^+ metabolism enzymes is largely independent of exercise intensity since the salvage pathway enzymes *NMNAT1* and *NAMPT* were the only genes displaying differential expression between HIIT and MICT.

2.1.2. Exercise-induced gene expression of Preiss-Handler pathway enzymes is sex-dependent

Considering sex differences, we found significant time sex interaction effects for *NMNAT1* ($F_{2,98.39} = 5.40$, $P_{ANOVA} = 0.0059$) and *NADSYN1* ($F_{2,94.29} = 3.50$, $P_{ANOVA} = 0.034$). Both enzymes revealed higher gene expression in males compared to females 1 h after exercise (all $P < 0.01$; Fig. S4e). This sex-dependent gene expression of Preiss-Handler pathway enzymes adds to previous reports on immunological differences between males and females (Dunn et al., 2024; Klein and Flanagan, 2016). Of note, NMNAT1 catalyzes the transfer of adenosine monophosphate onto both, nicotinic acid mononucleotide and nicotinamide mononucleotide (see Fig. 1), suggesting that the sex differences found for *NMNAT1* may not only apply for Preiss-Handler pathway, but also for NAD^+ salvage pathway.

2.1.3. Acute exercise increases gene expression of NAD^+ metabolism enzymes in PBMCs

Given that time- and energy-matched HIIT and MICT revealed few intensity-dependent differences in PBMC gene expression, we pooled the results of both exercise conditions to increase statistical power for subsequent analyses of time effects. Linear mixed models and subsequent one-way ANOVAs revealed significant alterations over time for all analyzed genes (for full results see Supplementary Table S4 and S5). Pairwise comparisons of timepoints demonstrated distinct gene expression kinetics for different NAD^+ metabolism enzymes (Fig. 3b-d). Except for *QPRT*, all analyzed kynurenine and Preiss-Handler pathway enzymes revealed increased gene expression 1 h after exercise (Fig. 3b, c), suggesting that NAD^+ biosynthesis of PBMCs is predominantly maintained via these pathways during the post-exercise recovery phase. In contrast, a transient increase in gene expression was found immediately after exercise for *QPRT* ($P < 0.0001$) and the salvage pathway enzymes *NMRK1* ($P < 0.01$) and *NAMPT* ($P < 0.0001$; Fig. 3b, d). When comparing gene expression results immediately after exercise, *NAMPT*, the gene encoding for the rate-limiting enzyme of nicotinamide salvage, revealed a strong increase (mean fold change: 2.46 ± 0.72; Fig. 3d). A similar response was observed for *QPRT* (mean fold change: 2.87 ± 3.34; Fig. 3b), which encodes for the enzyme that incorporates quinolinic acid from the kynurenine pathway into the Preiss-Handler pathway. In contrast, *NMRK1* increased in a less pronounced manner (mean fold change: 1.27 ± 0.59; Fig. 3d), suggesting a predominant role of *NAMPT* and *QPRT* in the acute response to exercise. Underlining these findings, *NAMPT* and *QPRT* were the only genes that increased immediately after both HIIT and MICT when analyzing PBMC gene expression separated by exercise condition (all $P < 0.05$; Fig. S4a-c). Collectively, these results suggest that gene expression of NAD^+ metabolism enzymes of PBMCs is regulated by acute exercise with distinct expression patterns across different NAD^+ biosynthesis pathways. In line with previous research demonstrating the regulatory potential of NAD^+ metabolism in different immune cells (Fang et al., 2023), these observations shed light on a potential role of exercise in modifying immune cell metabolism.

2.1.4. Acute exercise increases protein abundance of NAD^+ salvage pathway enzymes in PBMCs

Concerning the evolutionary conservation of NAD^+ salvage pathway genes (Bieganowski and Brenner, 2004), and the transient but pronounced increase in *NAMPT* gene expression immediately after exercise, we hypothesized that NAD^+ salvage from nicotinamide – rather than biosynthesis from tryptophan, nicotinic acid, trigonelline, or nicotinamide riboside – might be integral to the exercise-induced regulation of NAD^+ metabolism of PBMCs. This prominence of nicotinamide salvage has previously been reported in different immunological contexts including viral defense (Holay et al., 2023) and anticancer immunity (Guo et al., 2023; Wang et al., 2021). We thus determined the intracellular protein abundance for NMNAT1 and NAMPT, the two core enzymes needed for NAD^+ salvage from nicotinamide (see Fig. 1). Linear mixed models and subsequent ANOVAs did not demonstrate any interaction effects for intracellular protein abundance of NMNAT1 and NAMPT in relation to exercise condition or sex (Supplementary Table S2 and S3). As for the gene expression results, we thus pooled the protein data to increase statistical power for subsequent analyses of time effects.

Confirming our hypothesis, one-way ANOVAs revealed significant alterations over time for NMNAT1 ($F_{2,106.86} = 7.33$; $P_{ANOVA} = 0.001$) and NAMPT ($F_{2,112.52} = 6.55$; $P_{ANOVA} = 0.002$) and pairwise comparisons showed a transient increase in intracellular protein abundance immediately after exercise for both enzymes (mean fold change for NMNAT1: 1.61 ± 1.28, $P < 0.01$; mean fold change for NAMPT: 1.41 ± 0.92, $P < 0.01$; Fig. 3e,f). These results demonstrate that the intracellular protein abundance of NAD^+ salvage pathway enzymes is transiently increased in response to acute exercise in PBMCs. While increased NAMPT gene expression was mirrored by higher protein abundance (Fig. 3d,f), the gene and protein data for NMNAT1 suggest post-transcriptional mechanisms (Fig. 3c,f).

Collectively, we show that time- and energy-matched HIIT and MICT trigger similar alterations in gene expression and protein abundance of NAD^+ metabolism enzymes of PBMCs with minor differences between males and females. Acute exercise causes distinct, pathway-specific alterations in gene expression with protein abundance of NAD^+ salvage pathway enzymes transiently increasing immediately after exercise. Similar to previous reports that NAD^+ salvage pathway is central to immune cell metabolism and function (Holay et al., 2023; Guo et al., 2023; Wang et al., 2021; Fang et al., 2023), this exercise-induced reorganization of NAD^+ metabolism might foster energy-intensive processes

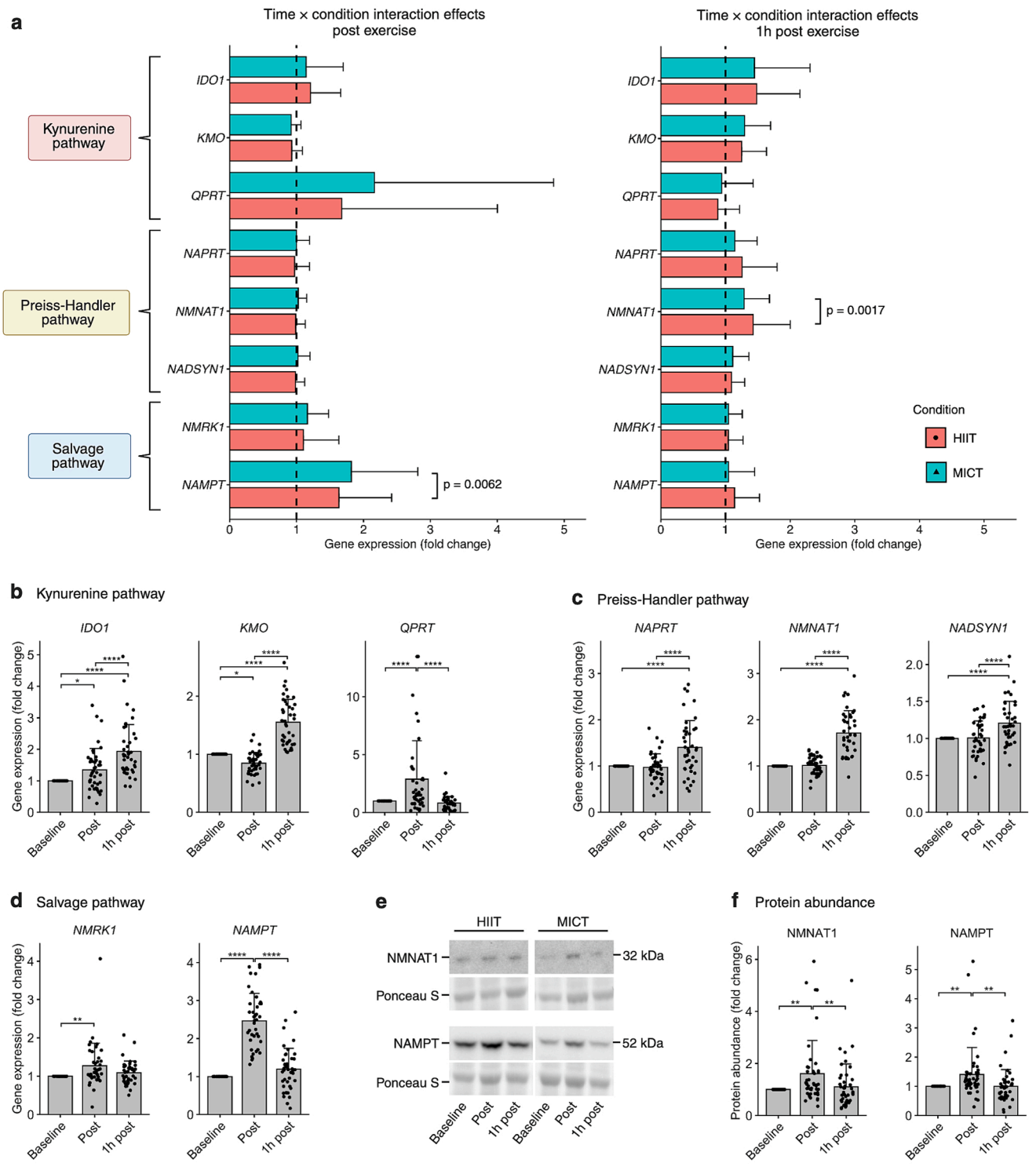

Fig. 3. Acute exercise boosts gene expression and protein abundance of NAD$^+$ metabolism enzymes in PBMCs. (a) Gene expression of key NAD$^+$ metabolism enzymes in response to HIIT and MICT (N = 22). Linear mixed models with exercise condition, sex, and time as fixed effects were employed. For significant ANOVA time*condition interaction effects, pairwise comparisons of HIIT and MICT were performed for each timepoint. (b-d) Exercise-induced alterations in gene expression of kynurenine pathway (b), Preiss-Handler pathway (c), and salvage pathway enzymes (d) over time (N = 44). (e,f) Representative examples of Western Blots (e) and overall protein abundance (f) of the salvage pathway enzymes NMNAT1 and NAMPT in response to exercise. Full Western Blot membranes are appended in Fig. S5. Linear mixed models with subsequent one-way repeated measures ANOVAs were employed. For significant ANOVA time effects, pairwise comparisons of timepoints were performed (* $P < 0.05$; ** $P < 0.01$; *** $P < 0.001$; **** $P < 0.0001$). All displayed values are mean ± standard deviation. A full depiction of the dataset including baseline variability is given in Fig. S6.

such as immune cell migration, infiltration into target tissues, and elevated immune effector function, which are commonly observed in response to exercise (Campbell and Turner, 2018; Rumpf et al., 2021).

2.2. Temporal regulation of NAD^+ metabolism during exercise in PBMCs (trial 2)

To characterize the impact of exercise on NAD^+ metabolism of PBMCs in greater detail, we made use of a longitudinal exercise trial with high temporal resolution (Fig. 2b). We recruited 12 healthy participants (6 female) of similar age but lower cardiorespiratory fitness than in trial 1 (for in- and exclusion criteria see Supplementary Table S6). This enabled us to assess whether alterations in NAD^+ metabolism of PBMCs were also present in less trained individuals. Participants exhibited a mean VO_{2peak} of 45.42 ± 9.65 mL min^{-1} kg^{-1} (Fig. S7a), which is about 10 mL lower than in trial 1 and just above the 70th percentile compared to age- and sex-matched reference values (Kaminsky et al., 2022). Detailed participant characteristics are displayed in Table 2. Participants performed a single exercise session on a bicycle ergometer, and PBMCs and blood serum were isolated at a total of eight timepoints between baseline and 1 h after exercise (Fig. 2b). Similar to trial 1, interindividual variation, expressed as overall mean CV was 25.58 % (for detailed CVs see Fig. S3d-g). We also recorded breath-by-breath respiratory data during the exercise session to monitor the participants' internal load in real time during the exercise bout. Overall, participants achieved a mean exercise intensity of 66.48 ± 8.53 % VO_{2peak} and a mean respiratory exchange ratio of 0.93 ± 0.04 (Fig. S7b,c).

2.2.1. Increased NAMPT gene expression during acute exercise

To characterize the precise gene expression kinetics of NAD^+ metabolism enzymes in response to exercise, we analyzed the same set of genes as in trial 1 (see enzymes highlighted in green in Fig. 1). Linear mixed models and subsequent one-way ANOVAs revealed significant alterations over time for six of the eight analyzed genes (Fig. 4a-c; Supplementary Table S7 and S8). Interestingly, *NAMPT* was the only gene that revealed increased gene expression during exercise (highest mean fold change: 6.56 ± 6.19; $F_{7,77} = 6.38$; $P_{ANOVA} = 6.34 \times 10^{-6}$). In contrast, all other genes decreased (all $P_{ANOVA} < 0.05$). Of note, we obtained similar results when performing linear mixed models and one-way ANOVAs without the last measurement timepoint (i.e., 1 h post exercise), indicating that the observed time effects were attributable to alterations in gene expression which occurred during the exercise session, as opposed to the subsequent recovery period (see Supplementary Table S9 and S10). In line with the gene expression and protein abundance observed in trial 1, these results suggest that NAD^+ metabolism of PBMCs is shifted towards nicotinamide salvage rather than *de novo* synthesis or use of other NAD^+ precursors during acute exercise. Mechanistically, the elevated *NAMPT* expression observed during exercise might be explained by a cellular signaling cascade involving sirtuin 1 (SIRT1), circadian locomotor output cycles protein kaput (CLOCK), and basic helix-loop-helix ARNT-like protein (BMAL) 1. SIRT1/CLOCK:BMAL1 signaling maintains intracellular NAD^+ levels by coupling the local abundance of NAD^+ to the expression of *NAMPT*, a mechanism which is shared across various tissues for the circadian regulation of NAD^+ levels (Basse et al., 2023; Sato and Sassone-Corsi, 2022). Exercise-induced changes in metabolic activity might trigger the same signaling cascade, thereby adjusting intracellular NAD^+ levels of PBMCs to the increased metabolic demand resulting from sympathetic activation (Walzik et al., 2023).

2.2.2. Acute exercise increases NAD^+ levels of PBMCs

Against the backdrop of increased NAMPT gene expression and protein abundance in response to exercise (Fig. 3d-f; Fig. 4c), we next hypothesized that this would create a metabolic demand for nicotinamide, the direct substrate of NAMPT (Fig. 1). NAMPT displays a high affinity for nicotinamide with K_M values ranging from 0.92 to 1.24 μM (Revollo et al., 2004; Rongvaux et al., 2002), suggesting that exercise-triggered NAMPT expression would drive this reaction via canonical enzyme induction. To test this hypothesis, we performed targeted metabolomics on PBMC lysates. Surprisingly, intracellular concentrations of nicotinamide and other NAD^+ precursors such as tryptophan, kynurenine, or nicotinamide riboside remained unaltered in response to exercise (Fig. 4e, for full results of linear mixed models and ANOVAs see Supplementary Table S7 and S8). However, NAD^+ levels revealed a significant increase over time ($F_{3,26.53} = 3.75$; $P_{ANOVA} = 0.023$; Fig. 4d). To preclude that NAD^+ levels increased due to a shift in NAD^+/NADH redox status, we also determined intracellular NADH levels and calculated NAD^+/NADH ratios. Interestingly, no significant changes were found for NADH ($F_{3,26.41} = 2.25$; $P_{ANOVA} = 0.106$) and the NAD^+/NADH ratio ($F_{3,25.98} = 0.79$; $P_{ANOVA} = 0.509$; Fig. 4d), suggesting elevated NAD^+ biosynthesis in PBMCs in response to exercise. These results complement our previous findings on increased NAMPT gene expression and protein abundance and support the hypothesis that NAMPT plays a crucial role in NAD^+ biosynthesis of PBMCs in response to exercise.

2.2.3. Serum levels of the NAD^+ precursor nicotinamide are diminished by acute exercise

Inspired by previous reports that nicotinamide is a critical contributor to NAD^+ biosynthesis across various tissues (Liu et al., 2018), we next hypothesized that serum levels of nicotinamide were altered by exercise. Indeed, we found a continuous decrease in serum concentrations of nicotinamide from 340 ± 157 nM at baseline to 185 ± 83 nM 1 h after exercise (mean delta nicotinamide: 154 nM; $F_{7,76.01} = 13.02$; $P_{ANOVA} = 6.85 \times 10^{-11}$; Fig. 4f). In contrast, no alterations in serum concentrations were found for the NAD^+ precursor tryptophan ($F_{7,77} = 0.51$; $P_{ANOVA} = 0.824$) or for the catabolic end-product of NAD^+ metabolism N1-methylnicotinamide ($F_{7,77} = 1.5$; $P_{ANOVA} = 0.179$; Fig. 4f). Given that nicotinamide crosses cell membranes via simple diffusion, these results suggest nicotinamide uptake by different target tissues in response to exercise. A possible link to NAD^+ metabolism of PBMCs might be that higher NAMPT expression increases salvage pathway flux towards NAD^+, thereby creating a concentration gradient for nicotinamide across PBMC plasma membranes. This concentration gradient is

Table 2
Participant characteristics of trial 2.

	Overall ($N = 12$)			Female ($N = 6$)			Male ($N = 6$)		
	Min	Max	Mean ± SD	Min	Max	Mean ± SD	Min	Max	Mean ± SD
Age [years]	21	30	25.5 ± 2.71	21	30	24.67 ± 3.39	24	29	26.33 ± 1.75
Height [cm]	161	189.2	173.81 ± 9.43	161	181	167.45 ± 8.57	175.3	189.2	180.17 ± 5.0
Weight [kg]	45.1	96.3	69.75 ± 14.7	45.1	69.7	58.08 ± 8.21	71.1	96.3	81.42 ± 9.01
BMI [kg m^{-2}]	17.1	27.06	22.87 ± 3.12	17.1	24	20.7 ± 2.46	22.21	27.06	25.04 ± 2.01
RPE_{max} [A.U.]	17	20	18.83 ± 1.12	17	20	18.67 ± 1.21	17	20	19 ± 1.1
VO_{2peak} [mL kg^{-1} min^{-1}]	31	57	45.47 ± 9.65	31	46	37.76 ± 6.26	44	57	53.18 ± 4.79
HR_{max} [min^{-1}]	173	192	185.67 ± 6.06	181	186	183.33 ± 2.52	173	192	186.83 ± 7.17

Data is displayed for the entire study population and separated by sex.

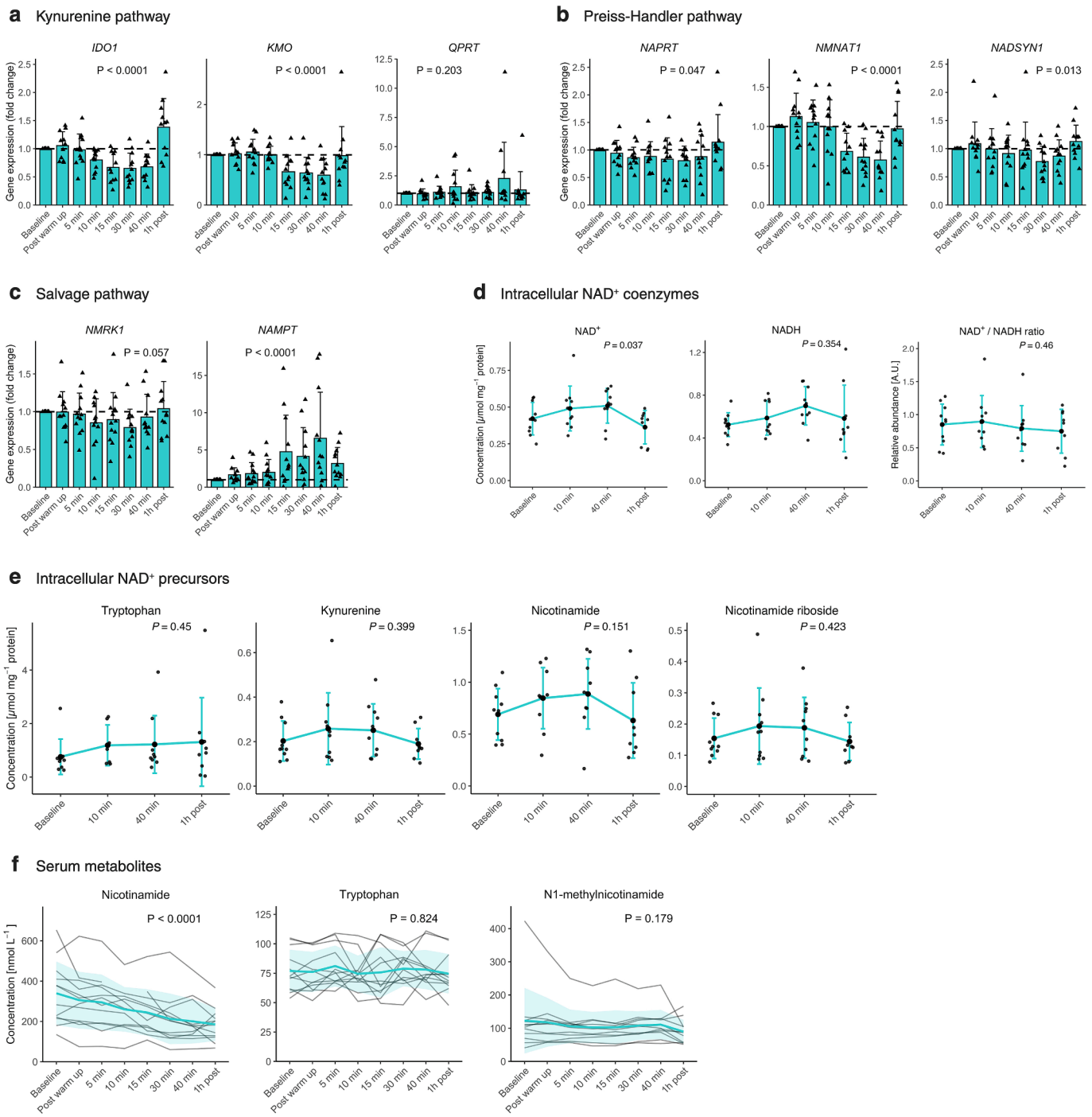

Fig. 4. High temporal resolution suggests NAD$^+$ salvage pathway as a crucial regulator of intracellular NAD$^+$ levels in response to exercise. a-c Gene expression of kynurenine pathway (a), Preiss-Handler pathway (b), and salvage pathway enzymes (c). d,e Intracellular levels NAD$^+$ coenzymes (d) and NAD$^+$ precursors (e). f Serum levels of NAD$^+$-related metabolites. Linear mixed models and one-way repeated measures ANOVAs were employed. All values are mean ± standard deviation. A full representation of all gene expression data including the baseline variability is given in Fig. S6.

alleviated by diffusion of nicotinamide from the blood plasma into PBMCs, resulting in decreased serum nicotinamide levels but unaltered intracellular concentrations. To causally prove this hypothesis, however, cell culture experiments on PBMCs are needed.

2.2.4. *High ATP levels may support NAMPT activity in PBMCs*

A further line of evidence for the exercise-induced regulation of NAD$^+$ metabolism arises from reports that the affinity of NAMPT for its substrates (nicotinamide and 5-phosphoribosyl 1-pyrophosphate) is strongly dependent on intracellular ATP levels (Hara et al., 2011). We found a significant increase in intracellular concentrations of ATP ($F_{3,24.49} = 8.33$; $P_{ANOVA} = 0.0005$; Fig. S8), which might have facilitated nicotinamide salvage. Besides ATP, we found alterations in several other intracellular metabolites such as ADP ($F_{3,23.79} = 4.7$; $P_{ANOVA} = 0.01$), and intermediates of ATP catabolism like inosine ($F_{3,25.86} = 9.05$; $P_{ANOVA} = 0.0003$) and hypoxanthine ($F_{3,25.26} = 6.81$; $P_{ANOVA} = 0.002$; Fig. S8). Similar to the exercise-induced regulation of NAD$^+$ metabolism, this suggests that ATP biosynthesis and breakdown of PBMCs are altered by acute exercise. Considering the crucial implications of ATP for cellular metabolism, this opens promising research avenues for future

investigations on the metabolic underpinnings of exercise-induced immune cell regulation.

3. Discussion

Here, we demonstrate in two complementary trials that NAD^+ metabolism of PBMCs is dynamically regulated by acute exercise. In a randomized crossover trial comparing time- and energy-matched HIIT and MICT, we reveal that exercise intensity only affects *NMNAT1* and *NAMPT* gene expression, but none of the other analyzed NAD^+ biosynthesis genes in PBMCs. Additionally, exercise-induced gene expression of Preiss-Handler pathway enzymes is sex-dependent, with higher values in males compared to females. Independent of exercise intensity, all analyzed genes revealed increased expression in response to exercise. While *NAMPT*, *NMRK1* and *QPRT* increased immediately after exercise, the remaining kynurenine and Preiss-handler pathway enzymes peaked in the subsequent recovery period. NAMPT and NMNAT1, the two core enzymes necessary for nicotinamide salvage, additionally displayed higher protein abundance immediately after exercise, suggesting a predominant role of the NAD^+ salvage pathway in the acute response to exercise. In a subsequent longitudinal exercise trial, we confirm these findings and reveal that *NAMPT* is the only gene that increases in expression during acute exercise, as opposed to the subsequent recovery period. Elevated *NAMPT* expression coincided with higher intracellular NAD^+ levels and diminished serum levels of the NAD^+ precursor nicotinamide, suggesting enhanced NAD^+ biosynthesis via nicotinamide salvage in PBMCs. These findings have broad implications for immunometabolism and immune effector function of PBMCs and might be of clinical relevance in different medical conditions linked to cellular immunity.

Given that NAD^+ is crucial for cellular energy metabolism, NAD^+-boosting strategies have attracted much scientific attention to treat conditions marked by disrupted NAD^+ homeostasis. These therapeutic approaches comprise pharmacological strategies such as inhibition of NAD^+-consuming enzymes or activation of NAD^+ biosynthetic enzymes (Covarrubias et al., 2021; Rajman et al., 2018), as well as non-pharmacological interventions such as diet, caloric restriction, supplementation with NAD^+ precursors, enhancing circadian rhythms, or exercise (Covarrubias et al., 2021). Of note, the translational evidence for potential health effects mediated by these NAD^+-boosting strategies differs considerably, although their mechanism of action is firmly established, respectively. For instance, it is well known that cellular NAD^+ levels are maintained via circadian expression of *NAMPT* (Sato and Sassone-Corsi, 2022; Nakahata et al., 2009; Ramsey et al., 2009), but boosting NAD^+ levels by improving circadian rhythms has not been investigated in humans so far. Similarly, exercise depicts a physiological stimulus that is known to impose metabolic stress on target cells and tissues, but outside of skeletal muscle tissue itself (Chubanava and Treebak, 2023; Costford et al., 2010; de Guia et al., 2019), it remains largely unknown whether exercise boosts NAD^+ levels (Walzik et al., 2023). As demonstrated here, acute exercise boosts NAD^+ metabolism of PBMCs, with potential implications in different immunological settings including viral defense, anticancer immunity, and immune-mediated anti-inflammatory adaptions.

In detail, it has repeatedly been demonstrated that viral infections such as SARS-CoV-2, Zika virus, or Epstein Barr virus infection dysregulate NAD^+ metabolism of infected cells and that pharmacological and nutritional modulation of NAD^+ metabolism depict therapeutic avenues to enhance antiviral response (Heer et al., 2020; Altay et al., 2021; Pang et al., 2021; Müller-Durovic et al., 2024; Izadpanah et al., 2023). Additionally, activation of bystander naïve $CD8^+$ T cells was dependent on NAD^+ salvage metabolism in response to virus exposure (Holay et al., 2023), underlining the central role of NAD^+ salvage in immune activation and viral defense. Our results obtained in response to a single exercise session suggest acute adaptions in NAD^+ metabolism of PBMCs, which might culminate in chronic adaptions, when acute exercise bouts are repeated regularly. For instance, it was shown for skeletal muscle that exercise training increases NAMPT protein expression (Costford et al., 2010; de Guia et al., 2019), which mirrors our findings obtained in response to acute exercise in PBMCs. Given that cellular NAD^+ depletion is proposed as a general hallmark of viral infection (Brenner, 2022; Zheng et al., 2022), chronic adaptions in NAD^+ metabolism might equip trained individuals with a higher metabolic capacity to fight viral infections. These results are supported by investigations showing lower infection risk for pneumonia (Jae et al., 2021) and a less severe COVID-19 diseases course (Ekblom-Bak et al., 2021) in individuals with high cardiorespiratory fitness. However, detailed analyses on the impact of exercise training on NAD^+ metabolism of immune cells are prospect of future investigation.

Besides viral defense, our results may also be applicable to anticancer immunity. Cellular cytotoxicity against tumors is predominantly ensured by immune effector cells such as $CD8^+$ T cells or natural killer (NK) cells, both of which are strongly mobilized in response to acute exercise (Schlagheck et al., 2020; Hoffman-Goetz and Pedersen, 1994; Pedersen and Hoffman-Goetz, 2000). Animal models have demonstrated that exercise training increases $CD8^+$ T cell and NK cell counts in different cancers (Pedersen et al., 2016; Kurz et al., 2022), thus offering first mechanistic insights into the reduced cancer incidence and mortality observed with physical activity (Patel et al., 2019; Moore et al., 2016). Although these results have not been replicated in humans so far (Campbell et al., 2024; Fiuza-Luces et al., 2024), acute exercise was shown to increase NK cell cytotoxicity in humans (Rumpf et al., 2021) with similar results also obtained for $CD8^+$ T cells in rodents (Rundqvist et al., 2020). For both immune effector populations, cellular cytotoxicity depends on NAD^+ metabolism (Guo et al., 2023; Wang et al., 2021; Wan et al., 2023), which sheds light at potential anticancer implications of our results. In detail, increased NAMPT expression and higher NAD^+ levels observed in PBMCs in response to exercise, might support immune effector function and cellular cytotoxicity against tumors.

Finally, clinical implications of the results obtained here also originate from studies employing supplementation with NAD^+ precursors as NAD^+-boosting strategy. NAD^+ precursors have received much scientific attention (Katsyuba et al., 2020; Rajman et al., 2018) and hold therapeutic value in numerous diseases including cardiovascular (Shi et al., 2024; Abdellatif et al., 2021), neurodegenerative (Brakedal et al., 2022), and metabolic conditions (Mouchiroud et al., 2013; Elhassan et al., 2017) as well as ageing per se (Covarrubias et al., 2021). In detail, seven clinical trials have demonstrated anti-inflammatory effects of nicotinamide riboside supplementation, many of which were mediated by altered cytokine expression of immune cells (Wang et al., 2022; Zhou et al., 2020; Han et al., 2023; Wu et al., 2022; Brakedal et al., 2022; Elhassan et al., 2019; Remie et al., 2020). Since nutritional modulation of NAD^+ metabolism modified immune cell function in these trials, similar anti-inflammatory effects might also be suspected for the acute exercise-induced alterations in NAD^+ metabolism observed here. In fact, although acute exercise depicts a pro-inflammatory stimulus (Immune function and exercise, 2011), chronic exercise training exerts anti-inflammatory effects, which are integral to disease prevention and treatment (Gleeson et al., 2011). Thus, our results open promising research avenues on the impact of exercise-induced alterations in NAD^+ metabolism for immune-mediated health effects. Such investigations could also hold value in the context of inflammageing and immunosenescence, which are characterized by reduced NAD^+ levels and increased pro-inflammatory cytokine expression (Covarrubias et al., 2020; Chini et al., 2020). For instance, macrophage NAD^+ biosynthesis is integral to immune function in ageing and inflammation (Minhas et al., 2019), which emphasizes the interconnection of NAD^+ metabolism and immune function in pathophysiological cell states.

In summary, we demonstrate in two complementary trials that NAD^+ metabolism of PBMCs is regulated by acute exercise in a pathway-specific manner. Increased gene expression and protein abundance of NAMPT, the rate-limiting enzyme of nicotinamide salvage, was

accompanied by elevated NAD^+ levels, with potential implications for immune cell metabolism and function. In a broader context, this metabolic reorganization of NAD^+ metabolism could equip immune cells with a higher metabolic capacity for energy-intensive processes such as transmigration from the blood into target tissues and elevated effector function, both of which are commonly observed with exercise. Since these immunological mechanisms are integral to antiviral response, anticancer immunity, and the amelioration of inflammatory conditions, an improved understanding of the metabolic underpinnings of exercise-induced immune cell trafficking holds promise in elucidating the health-promoting effects of exercise in disease prevention and treatment. To elaborate on these findings, randomized controlled trials with healthy and diseased populations are needed. In dependence on the precise research question, such trials could benefit of distinguishing different immune cell populations to enable a metabolic and functional characterization of specific immune cells in response to exercise. Taking this approach could ultimately elucidate the molecular underpinnings of immune-mediated health effects and thus allow for evidence-based exercise recommendations in clinical settings.

4. Material and methods

Both trials reported on here meet the National Institutes of Health definition of a clinical trial and received approval by a local ethics committee, which worked according to the World Medical Association's Declaration of Helsinki, respectively. The first trial was a randomized crossover trial approved by the ethics committee of the German Sport University Cologne and conducted between October 2019 and September 2020. The second trial was a longitudinal exercise trial approved by the ethics committee of the Leibniz Research Centre for Working Environment and Human Factors at Dortmund University and conducted between June and October 2022. Prospective registration in the German Clinical Trials Register was performed for trial 1 (DRKS00017686) and trial 2 (DRKS00029105).

4.1. Randomized crossover trial (trial 1)

In total, 24 healthy adults (12 males) were included in a randomized crossover trial (Fig. S1). We decided to recruit recreationally active runners with a minimum weekly training duration of 3–5 h to ensure that participants were familiar with treadmill running and capable of completing the high-intensity intervals. Participants were scheduled for a total of three visits to an exercise physiology laboratory at the German Sport University Cologne and were instructed to arrive fasted and to refrain from caffeine and alcohol intake in the 24 h prior to each visit. Water intake was permitted ad libitum during all visits. All assessments were performed between 07:00 and 10:00 AM to account for a potential circadian impact on physiological and biological outcomes. In the initial baseline visit, written informed consent was obtained and anthropometric and demographic characteristics were recorded. Subsequently, cardiopulmonary exercise testing was performed.

4.1.1. Cardiopulmonary exercise testing

To determine the participants' VO_{2peak}, CPET was performed on a motorized treadmill (Woodway ELG 90, Weil am Rhein, Germany). The incline of the treadmill was set to 1 % for all exercise sessions. After a warm-up period of 5 min at 6–8 km/h, participants began running on the treadmill at 8 km/h. Exercise intensity was then increased by 1 km/h every 60 s until volitional exhaustion. Rate of perceived exertion was recorded every minute and verbal encouragement was given by the supervising researcher. Following a 5-minute break, a VO_{2peak} verification test at 1 km/h faster than the last stage was performed. The speed was increased to the desired velocity within 20 s and participants were instructed to run as long as they could. During the CPET, participants wore a mask that was connected to a spirometer (Cortex Metalyzer 3B, CORTEX Biophysik GmbH, Leipzig, Germany) to collect breathing gases breath-by-breath. VO_{2peak} was calculated as the mean of the highest 15-second interval during CPET. After completion of the baseline visit participants were randomized into one of two intervention sequences: HIIT-MICT or MICT-HIIT. Randomization was performed by concealed allocation (1:1) using the software Randomization in Treatment Arms (RITA; Evident, Lübeck, Germany). Following the minimization procedure according to Pocock and Simon (Scott et al., 2002), BMI, VO_{2peak}, and age were used as stratification factors for randomization.

4.1.2. Interventions and blood sampling

To prevent carryover effects between the exercise bouts performed at the three visits, the minimum timeframe between each visit was 72 h. For MICT participants ran on a treadmill (Woodway ELG 90, Weil am Rhein, Germany) for 50 min at 70 % of the VO_{2peak} determined during CPET. MICT was preceded by a 10-minute warm-up at a self-selected intensity. After a 5-minute break the 50-minute exercise session began. HIIT consisted of a 7-minute warm-up and a 7-minute cool-down on a treadmill (Woodway ELG 90, Weil am Rhein, Germany) at a running speed corresponding to 70 % VO_{2peak}. The exercise session comprised six 3-minute bouts of running at 90 % VO_{2peak} separated by 3 min of active recovery at 50 % VO_{2peak}. This exercise protocol was used to match HIIT and MICT for exercise duration and energy expenditure, as previously described (Bartlett et al., 2012). Thus, exercise intensity was the only diverging factor between HIIT and MICT. Venous blood samples were drawn before, immediately after, and 1 h after HIIT and MICT from a median cubital vein and in a supine position. After serum and PBMC isolation, samples from this trial were used to assess gene expression and protein abundance of NAD^+ biosynthetic enzymes (see analytic procedures).

4.2. Longitudinal exercise trial (trial 2)

In total, 12 healthy adults (6 males) were included in the longitudinal exercise trial (Fig. S2). To assess whether exercise-induced alterations in NAD^+ metabolism of PBMCs are also observed in recreationally active adults, we recruited less physically active individuals compared to trial 1. In- and exclusion criteria for participation in this trial are displayed in Supplementary Table S4. Participants visited an exercise physiology laboratory of TU Dortmund University for a total of 2 visits. All analyses were conducted between 08:00 and 10:00 AM to account for any influence of circadian rhythm on physiological and biological outcomes. Participants were asked to appear in a fasted state to each of the visits and refrain from physical activity, alcohol consumption, and caffeine intake in the 48 h prior. During an initial baseline visit, written informed consent was obtained, anthropometric and demographic characteristics were recorded, and CPET was conducted.

4.2.1. Cardiopulmonary exercise testing

To avoid underachievement in the CPET due to lack of experience in treadmill running, participants of this trial performed the CPET on a stationary bicycle ergometer (ergoselect 5, ergoline GmbH). After a 2-min warm-up of unloaded pedaling, participants performed a ramp protocol with increasing intensity (15–30 Watts/min depending on sex, BMI, and physical activity level) until volitional exhaustion. Afterwards, participants performed an unloaded cool-down for 3 min. During the CPET, participants wore a mask that was connected to a spirometer (Cortex Metalyzer 3B, CORTEX Biophysik GmbH, Leipzig, Germany) to collect breathing gases breath-by-breath. VO_{2peak} was calculated as the mean of the highest 15-second interval during CPET. Individual VO_2 kinetics of the CPET are displayed in Fig. S7a.

4.2.2. Intervention and blood sampling

The timeframe between the first and second visit was $\geq$ 72 h to prevent any carryover effects from the CPET to the exercise intervention. The exercise session during the second visit was performed on the same stationary bicycle ergometer as the CPET during the first visit

(ergoselect 5, ergoline GmbH). Participants performed a 5-minute warm-up at 15 % peak power output (PPO), followed by 40 min of cycling at 60 % VO_{2peak}, and a 3-minute cool-down at 15 % PPO. An intravenous cannula was placed in a superficial vein on the anterior portion of the forearm before the exercise session and venous blood samples were drawn before exercise, immediately after the warm-up, after 5, 10, 15, and 30 min of exercise, immediately after the exercise session as well as 1 h after the exercise session. Samples from this trial were used to assess gene expression of NAD^+ biosynthetic enzymes at high temporal resolution. Additionally, serum and intracellular NAD^+ metabolites were quantified.

4.3. Analytic procedures

4.3.1. Serum and PBMC isolation

Blood serum was collected in serum tubes. After 15 min of clotting, serum samples were centrifuged at 2,500xg for 10 min. Serum was then aliquoted and stored at −80 °C until further analysis. PBMCs were isolated from EDTA blood. After the blood draw, EDTA samples were diluted with PBS and carefully layered on top of a lymphocyte separation medium (BioWest, Lymphosep, Lymphocyte Separation Media L0560). Samples were then centrifuged at 1,200xg for 15 min. The PBMC-containing layer was separated and washed with PBS. Afterwards, cells were frozen at −150 °C until further analysis.

4.3.2. Quantitative Real-Time PCR (qRT PCR)

Using a column-based isolation kit (Promega GmbH, Germany), RNA was isolated from PBMCs. Concentration and purity on RNA isolates was measured on a Nanodrop™ microvolume spectrophotometer (Thermo Fisher Scientific, USA) and immediately used for cDNA synthesis (Promega GmbH, Germany). qRT PCR was performed for *IDO1, KMO, QPRT, NAPRT, NMNAT1, NADSYN1, NMRK1, and NAMPT* in relation to the reference genes *ACTB, RPS18* and *UBE2D2* using a PCR master mix (Promega GmbH, Germany) on a CFX96 Detection System (Bio-Rad Laboratories GmbH, Germany). Primers were either obtained from publications or designed in-house to span exon-exon-junctions. Primer details are displayed in Supplementary Table S11. Respecting PCR efficiency, relative gene expression compared to baseline was calculated using the ΔΔCt method. All gene expression results are reported as fold changes compared to baseline.

4.3.3. Western Blotting

Before Western Blotting, PBMCs were thawed, pelleted and resuspended in a lysis buffer containing RIPA buffer, 10 nM NaF, 1 mM Na3VO4, complete EDTA free protease inhibitor (Merck), Phospho Stop (Merck), 250U/ml Benzonase, and 10U/ml DNase 1. Cells were suspended in this lysis buffer for 1 h on ice and centrifuged at 13,000xg for 15 min afterwards. The supernatant was then transferred to a new tube for quantification of protein concentration using the PierceTM BCA Protein Assay Kit (Thermo Fischer). Cell lysates were stored at −80 °C until further analysis. In preparation for Western Blotting, PBMCs lysates were thawed, and lysates were diluted to a protein concentration of 2 mg/ml, suspended in 4x Laemmli buffer (#1610747; BioRad Laboratories GmbH, Munich, Germany) and heated at 95 °C for 1 min. 15 µg of protein were loaded on a 26-well 4–12 % BIS-TRIS Gel for each subject and time point. Using a gel-casting system in MOPS electrophoresis buffer, electrophoretic separation was conducted (all BioRad Laboratories GmbH, Munich, Germany). The gel was then transferred to a polyvinylidene difluoride (PVDF) membrane (GE Healthcare Life Science, Amersham, UK) by semidry blotting (Trans Blot Turbo, Bio-Rad, Hercules, CA, USA) for 40 min (1.2 A, 25 Vmax). By staining the PVDF membrane with Ponceau S, equal sample loading and transfer was checked. The membranes were then blocked for one hour at room temperature (RT) using 5 % nonfat dry milk dissolved in tris-buffered saline, which was supplemented with 0.1 % Tween20 (TBST). Primary antibodies dissolved in 5 % bovine serum albumin in TBST were incubated overnight at 4 °C for 17 h. The membranes were washed with TBST and incubated for one hour at RT with secondary antibodies diluted in TBST containing 5 % nonfat dry milk. After several washing steps, membranes were incubated with an enhanced chemiluminescence assay (ECL-Kit, GE Healthcare Life Science, Amersham, UK) for 3 min. Digital images of the responsive bands were automatically captured via an imaging system (ChemiDoc MP, Bio-Rad, Hercules, CA, USA). The membranes were then stripped for 6 min at RT using a Restore Western Blot Stripping Buffer (#21059; Thermo Scientific, Waltham, MA, USA). After blocking, they were incubated with primary antibodies for detection of proteins with different molecular weights and processed as described above. Band densities were assessed semi-quantitatively using ImageJ (v. 1.53 t; National Institute of Health, New York, NY, USA). Differences in densities between each band and Ponceau S were calculated for all timepoints and are expressed as fold change relative to baseline. Primary antibodies used for Western Blotting comprised NMNAT1 (rabbit polyclonal igG AB; #PA5-84418; 1:1000; Invitrogen, Regensburg, Germany) and NAMPT (mouse monoclonal igG1 AB; #MA5-43719; 1:2000; Invitrogen, Rockford, IL, USA). Secondary antibodies comprised HRP-linked anti-rabbit IgG (#7074S; 1:7500; Cell Signaling Technology, Danvers, MA, USA) and HRP-linked anti-mouse IgG (#7076S; 1:7500; Cell Signaling Technology, Danvers, MA, USA).

4.3.4. Liquid chromatography–tandem mass spectrometry (LC-MS/MS)-based targeted metabolomics

Serum concentrations of nicotinamide, tryptophan, and N1-methylnicotinamide were measured by LC-MS/MS as described previously (Midttun et al., 2009) at the Bevital laboratory (https://bevital.no). The lower limit of detection (LOD) for the assay ranged from 0.01 to 8 nmol/L. Within- and between-day coefficients of variation (CVs) ranged from 3 % to 8 % and 4 % to 10 %, respectively. Intracellular metabolites were quantified by high performance LC-MS/MS as previously described (Hiefner et al., 2023). Briefly, cell pellets were thawed on ice and spiked with $^{13}C_6$-nicotinamide (#V-034; Merck, Darmstadt, Germany). Metabolites were extracted by mixing the sample with pre-cooled acetonitrile/water 8:2 (v/v) and vortexing thoroughly at highest level for 1 min. Following homogenization, samples were incubated for 10 min on ice and centrifuged at 4 °C and 16,000xg for 10 min. The supernatants were transferred to a brown glass vial (#AR0-3741-13; Phenomenex, Torrance, CA, USA) and tightly closed with a crimped cap (LABSOLUTE®; Th. Geyer, Renningen, Germany). The extracts were measured immediately after extraction using a triple quadrupole mass spectrometer (QTRAP® 5500; SCIEX, Framingham, MA, USA) coupled to an ultra-high pressure liquid chromatography system (Nexera X2; Shimadzu, Kyoto, Japan). Analytes were separated by HILIC using a Luna® HPLC column (3 µm NH2 100 Å 150 mm × 2 mm, Phenomenex, Torrance, CA, USA). Solvent A contained 20 mM ammonium acetate in MS-grade water (pH 9.8) and solvent B contained 100 % acetonitrile. The flow rate was set to 0.25 mL/min with a linear gradient of decreasing solvent B (0–17 min, 80 %-0%), followed by 8 min at 0 % solvent B and 5 min re-equilibration at 80 % solvent B. The MS was equipped with an ESI source and all measurements were carried out in negative ionization and multiple reaction monitoring (MRM) scan mode. Data analysis was performed using SCIEX OS software and by manual quantification in Microsoft Excel. Analyte peaks were identified based on MRM transitions and retention time as given in ref. (Hiefner et al., 2023). A standard calibration curve ranging from 2 nM to 20 µM was used for accurate quantification and all analyte peak areas were normalized against internal standard peak areas. Calculated NAD^+ metabolite concentrations were normalized against protein determined by the Pierce™ BCA Protein Assay Kit (#23225; Thermo Scientific, Rockford, IL, USA) according to the manufactureŕs protocol.

4.4. Data processing and statistical analyses

All data obtained in trial 1 and 2 were assessed for missing values and

experimental/technical outliers before starting statistical analyses. In trial 1 6.16 % of the gene expression data were missing (for reasons see Supporting file 1). Subsequently, fold changes relative to baseline were calculated, data was z-transformed and values ≥ 3 standard deviations were deleted. This resulted in deletion of another 1.27 % of the gene expression data. For Western Blot data three values (1.09 %) were missing and one value (0.36 %) was deleted since it resulted to be negative after calculation of the relative protein abundance compared to Ponceau S staining. Z-transformation of the calculated fold changes did not show any outliers in the Western Blot data, and we thus refrained from deleting any data points. A full summary of missing values and a summary of the values removed after z-transformation is given in Supporting File 1.

In trial 2, three values (0.39 %) were missing in the gene expression data. After calculating fold changes, gene expression data was z-transformed and analyzed for outliers ≥ 3 standard deviations. In total, two further values (0.26 %) were deleted before performing statistical analyses. Serum metabolites and intracellular metabolites revealed one missing value (0.35 %) 83 missing values (11.79 %), respectively. Z-transformation yielded no outliers ≥ 3 standard deviations and statistical analysis was thus performed without further deletion of any data points. A full summary of missing values and a summary of the values removed after z-transformation is given in Supporting File 1.

All datasets were then analyzed using the R packages lme4, lmerTest, and emmeans. In trial 1, linear mixed models were calculated for each outcome using time and exercise condition as fixed effects and the participant ID as random effect (fold change from baseline ~ Timepoint * Condition + (1 | ID)). The results of the linear mixed models were then used to perform analyses of variance. In case of significant time and/or time*exercise condition interaction effects, pairwise comparisons of timepoints and/or exercise conditions were performed. Sex differences were analyzed in the same manner but with sex as a fixed effect. Time effects on the pooled dataset of trial 1 and data from trial 2 were analyzed using time as a fixed effect and participant ID as a random effect (fold change from baseline ~ Timepoint + (1 | ID)). Level of significance for all statistical tests was set to $\alpha = 0.05$. An overview of all statistical results is given in Supplementary Table S2 – S10.

Author contributions

D.W. contributed to data preparation and cleaning, performed statistical analyses, created figures and tables, and wrote the original draft of the manuscript. N.J. conceptualized and supervised trial 2, contributed to data preparation and cleaning, and gave intellectual input. A.S. performed gene expression analyses. S.T. conducted trial 2. A.J.M. Conceptualized, supervised, and conducted trial 1. K.S. and S.G. performed Western Blot analyses. P.S. performed data preparation and cleaning. P.M.U. and A.M. performed serum metabolomics. J.H. and A. W. performed intracellular metabolomics. C.B. provided intellectual input. C.W. provided intellectual input, laboratory equipment and experimental resources. P.Z. conceptualized and supervised trial 1 and 2 and provided intellectual input. All authors reviewed and edited the original draft and approved the final version of the manuscript before submission

CRediT authorship contribution statement

David Walzik: Writing – original draft, Visualization, Investigation, Formal analysis, Data curation. **Niklas Joisten:** Writing – review & editing, Supervision, Project administration, Formal analysis, Data curation, Conceptualization. **Alexander Schenk:** Writing – review & editing, Methodology. **Sina Trebing:** Writing – review & editing, Investigation. **Kirill Schaaf:** Writing – review & editing, Methodology. **Alan J Metcalfe:** Writing – review & editing, Supervision, Investigation, Conceptualization. **Polyxeni Spiliopoulou:** Writing – review & editing, Data curation. **Johanna Hiefner:** Writing – review & editing, Methodology. **Adrian McCann:** Writing – review & editing, Methodology. **Carsten Watzl:** Writing – review & editing, Resources. **Per Magne Ueland:** Writing – review & editing, Methodology. **Sebastian Gehlert:** Writing – review & editing, Methodology. **Anna Worthmann:** Writing – review & editing, Methodology. **Charles Brenner:** Writing – review & editing. **Philipp Zimmer:** Writing – review & editing, Supervision, Conceptualization.

Funding

Internal funds of the German Sport University Cologne awarded to A. J.M. partly covered the costs of trial 1. C.B. was supported by R01HL127545 and the Alfred E. Mann Family Foundation.

Declaration of Competing Interest

The authors declare the following financial interests/personal relationships which may be considered as potential competing interests: C. B. serves as a scientific advisor and holds equity interests in ChromaDex, Alphina Therapeutics and Juvenis.

Acknowledgements

We would like to thank Lars Donath, Ludwig Rappelt, Tiffany Y. Wences Chirino, Lisa Heesen, Julia Dreilich, and Daniel Renpening for their support in conducting the trials. We also thank the German Sport University Cologne for supplying internal funds for trial 1 and the National Insitutes of Health and the Alfred E. Mann Family Foundation for supporting C.B..

Appendix A. Supplementary data

Supplementary data to this article can be found online at https://doi.org/10.1016/j.bbi.2024.11.004.

Data availability

The data generated during the two trials will be shared with researchers upon reasonable request. Requests will be reviewed by the corresponding author and any transfer of data and materials will be accompanied by a material transfer agreement.

References

Abdellatif, M., Sedej, S., Kroemer, G., 2021. NAD $^{+}$ metabolism in cardiac health, aging, and disease. Circulation 144, 1795–1817.

Altay, O., Arif, M., Li, X., Yang, H., Aydın, M., Alkurt, G., Kim, W., Akyol, D., Zhang, C., Dinler-Doganay, G., Turkez, H., Shoaie, S., Nielsen, J., Borén, J., Olmuscelik, O., Doganay, L., Uhlén, M., Mardinoglu, A., 2021. Combined metabolic activators accelerates recovery in mild-to-moderate COVID-19. Adv. Sci. 8, 2101222.

Bartlett, J.D., Hwa Joo, C., Jeong, T.-S., Louhelainen, J., Cochran, A.J., Gibala, M.J., Gregson, W., Close, G.L., Drust, B., Morton, J.P., 2012. Matched work high-intensity interval and continuous running induce similar increases in PGC-1α mRNA, AMPK, p38, and p53 phosphorylation in human skeletal muscle. J. Appl. Physiol. 112, 1135–1143.

A. L. Basse, K. N. Nielsen, I. Karavaeva, L. R. Ingerslev, T. Ma, J. F. Havelund, T. S. Nielsen, M. Frost, J. Peics, E. Dalbram, M. Dall, J. R. Zierath, R. Barrès, Z. Gerhart-Hines, NAMPT-dependent NAD+ biosynthesis controls circadian metabolism in a tissue-specific manner. 120 (2023).

Bieganowski, P., Brenner, C., 2004. Discoveries of Nicotinamide Riboside as a Nutrient and Conserved NRK Genes Establish a Preiss-Handler Independent Route to NAD+ in Fungi and Humans. Cell 117, 495–502.

Bogan, K.L., Brenner, C., 2008. Nicotinic Acid, Nicotinamide, and Nicotinamide Riboside: A Molecular Evaluation of NAD $^{+}$ Precursor Vitamins in Human Nutrition. Annu. Rev. Nutr. 28, 115–130.

Brakedal, B., Dölle, C., Riemer, F., Ma, Y., Nido, G.S., Skeie, G.O., Craven, A.R., Schwarzlmüller, T., Brekke, N., Diab, J., Sverkeli, L., Skjeie, V., Varhaug, K., Tysnes, O.-B., Peng, S., Haugarvoll, K., Ziegler, M., Grüner, R., Eidelberg, D., Tzoulis, C., 2022. The NADPARK study: a randomized phase I trial of nicotinamide riboside supplementation in Parkinson's disease. Cell Metab. 34, 396–407.e6.

Brenner, C., 2022. Viral infection as an NAD+ battlefield. Nat. Metab. 4, 2–3.

Campbell, J.P., Turner, J.E., 2018. Debunking the Myth of Exercise-Induced Immune Suppression: Redefining the Impact of Exercise on Immunological Health Across the Lifespan. Front. Immunol. 9, 648.

Campbell, J.P., Walzik, D., Zimmer, P., 2024. What dictates tumour cell sensitivity to exercise? Nat. Rev. Immunol. https://doi.org/10.1038/s41577-024-01001-z.

Chini, C.C.S., Peclat, T.R., Warner, G.M., Kashyap, S., Espindola-Netto, J.M., de Oliveira, G.C., Gomez, L.S., Hogan, K.A., Tarragó, M.G., Puranik, A.S., Agorrody, G., Thompson, K.L., Dang, K., Clarke, S., Childs, B.G., Kanamori, K.S., Witte, M.A., Vidal, P., Kirkland, A.L., De Cecco, M., Chellappa, K., McReynolds, M.R., Jankowski, C., Tchkonia, T., Kirkland, J.L., Sedivy, J.M., van Deursen, J.M., Baker, D.J., van Schooten, W., Rabinowitz, J.D., Baur, J.A., Chini, E.N., 2020. CD38 ecto-enzyme in immune cells is induced during aging and regulates NAD+ and NMN levels. Nat. Metab. 2, 1284–1304.

Chubanava, S., Treebak, J.T., 2023. Regular exercise effectively protects against the aging-associated decline in skeletal muscle NAD content. Exp. Gerontol. 173, 112109.

Costford, S.R., Bajpeyi, S., Pasarica, M., Albarado, D.C., Thomas, S.C., Xie, H., Church, T. S., Jubrias, S.A., Conley, K.E., Smith, S.R., 2010. Skeletal muscle NAMPT is induced by exercise in humans. Am. J. Physiol.-Endocrinol. Metab. 298, E117–E126.

Covarrubias, A.J., Kale, A., Perrone, R., Lopez-Dominguez, J.A., Pisco, A.O., Kasler, H.G., Schmidt, M.S., Heckenbach, I., Kwok, R., Wiley, C.D., Wong, H.-S., Gibbs, E., Iyer, S. S., Basisty, N., Wu, Q., Kim, I.-J., Silva, E., Vitangcol, K., Shin, K.-O., Lee, Y.-M., Riley, R., Ben-Sahra, I., Ott, M., Schilling, B., Scheibye-Knudsen, M., Ishihara, K., Quake, S.R., Newman, J., Brenner, C., Campisi, J., Verdin, E., 2020. Senescent cells promote tissue NAD+ decline during ageing via the activation of CD38+ macrophages. Nat. Metab. 2, 1265–1283.

Covarrubias, A.J., Perrone, R., Grozio, A., Verdin, E., 2021. NAD+ metabolism and its roles in cellular processes during ageing. Nat. Rev. Mol. Cell Biol. 22, 119–141.

de Guia, R.M., Agerholm, M., Nielsen, T.S., Consitt, L.A., Søgaard, D., Helge, J.W., Larsen, S., Brandauer, J., Houmard, J.A., Treebak, J.T., 2019. Aerobic and resistance exercise training reverses age-dependent decline in NAD $^+$ salvage capacity in human skeletal muscle. Physiol. Rep. 7. https://doi.org/10.14814/phy2.14139.

Di Stefano, M., Nascimento-Ferreira, I., Orsomando, G., Mori, V., Gilley, J., Brown, R., Janeckova, L., Vargas, M.E., Worrell, L.A., Loreto, A., Tickle, J., Patrick, J., Webster, J.R.M., Marangoni, M., Carpi, F.M., Pucciarelli, S., Rossi, F., Meng, W., Sagasti, A., Ribchester, R.R., Magni, G., Coleman, M.P., Conforti, L., 2015. A rise in NAD precursor nicotinamide mononucleotide (NMN) after injury promotes axon degeneration. Cell Death Differ. 22, 731–742.

Diguet, N., Trammell, S.A.J., Tannous, C., Deloux, R., Piquereau, J., Mougenot, N., Gouge, A., Gressette, M., Manoury, B., Blanc, J., Breton, M., Decaux, J.-F., Lavery, G. G., Baczkó, I., Zoll, J., Garnier, A., Li, Z., Brenner, C., Mericskay, M., 2018. Nicotinamide riboside preserves cardiac function in a mouse model of dilated cardiomyopathy. Circulation 137, 2256–2273.

Dunn, S.E., Perry, W.A., Klein, S.L., 2024. Mechanisms and consequences of sex differences in immune responses. Nat. Rev. Nephrol. 20, 37–55.

Ekblom-Bak, E., Väisänen, D., Ekblom, B., Blom, V., Kallings, L.V., Hemmingsson, E., Andersson, G., Wallin, P., Salier Eriksson, J., Holmlund, T., Lindwall, M., Stenling, A., Lönn, A., 2021. Cardiorespiratory fitness and lifestyle on severe COVID-19 risk in 279,455 adults: a case control study. Int. J. Behav. Nutr. Phys. Act 18, 135.

Elhassan, Y.S., Philp, A.A., Lavery, G.G., 2017. Targeting NAD+ in metabolic disease: new insights into an old molecule. J. Endocr. Soc. 1, 816–835.

Elhassan, Y.S., Kluckova, K., Fletcher, R.S., Schmidt, M.S., Garten, A., Doig, C.L., Cartwright, D.M., Oakey, L., Burley, C.V., Jenkinson, N., Wilson, M., Lucas, S.J.E., Akerman, I., Seabright, A., Lai, Y.-C., Tennant, D.A., Nightingale, P., Wallis, G.A., Manolopoulos, K.N., Brenner, C., Philp, A., Lavery, G.G., 2019. Nicotinamide riboside augments the aged human skeletal muscle NAD+ metabolome and induces transcriptomic and anti-inflammatory signatures. Cell Rep. 28, 1717–1728.e6.

Fang, E.F., 2019. Mitophagy and NAD+ inhibit Alzheimer disease. Autophagy 15, 1112–1114.

Fang, J., Chen, W., Hou, P., Liu, Z., Zuo, M., Liu, S., Feng, C., Han, Y., Li, P., Shi, Y., Shao, C., 2023. NAD+ metabolism-based immunoregulation and therapeutic potential. Cell Biosci 13, 81.

Fang, E.F., Scheibye-Knudsen, M., Chua, K.F., Mattson, M.P., Croteau, D.L., Bohr, V.A., 2016. Nuclear DNA damage signalling to mitochondria in ageing. Nat Rev Mol Cell Biol 17, 308–321.

Fang, E.F., Hou, Y., Palikaras, K., Adriaanse, B.A., Kerr, J.S., Yang, B., Lautrup, S., Hasan-Olive, M.M., Caponio, D., Dan, X., Rocktäschel, P., Croteau, D.L., Akbari, M., Greig, N.H., Fladby, T., Nilsen, H., Cader, M.Z., Mattson, M.P., Tavernarakis, N., Bohr, V.A., 2019. Mitophagy inhibits amyloid-β and tau pathology and reverses cognitive deficits in models of Alzheimer's disease. Nat. Neurosci. 22, 401–412.

Fiuza-Luces, C., Valenzuela, P.L., Gálvez, B.G., Ramírez, M., López-Soto, A., Simpson, R. J., Lucia, A., 2024. The effect of physical exercise on anticancer immunity. Nat. Rev. Immunol. 24, 282–293.

Gleeson, M., Bishop, N.C., Stensel, D.J., Lindley, M.R., Mastana, S.S., Nimmo, M.A., 2011. The anti-inflammatory effects of exercise: mechanisms and implications for the prevention and treatment of disease. Nat. Rev. Immunol. 11, 607–615.

Guo, X., Tan, S., Wang, T., Sun, R., Li, S., Tian, P., Li, M., Wang, Y., Zhang, Y., Yan, Y., Dong, Z., Yan, L., Yue, X., Wu, Z., Li, C., Yamagata, K., Gao, L., Ma, C., Li, T., Liang, X., 2023. NAD+ salvage governs mitochondrial metabolism, invigorating natural killer cell antitumor immunity. Hepatology 78, 468–485.

Han, K., Singh, K., Meadows, A.M., Sharma, R., Hassanzadeh, S., Wu, J., Goss-Holmes, H., Huffstutler, R.D., Teague, H.L., Mehta, N.N., Griffin, J.L., Tian, R., Traba, J., Sack, M.N., 2023. Boosting NAD preferentially blunts Th17 inflammation via arginine biosynthesis and redox control in healthy and psoriasis subjects. Cell Rep. Med. 4, 101157.

Hara, N., Yamada, K., Shibata, T., Osago, H., Tsuchiya, M., Oresic, M., 2011. Nicotinamide phosphoribosyltransferase/visfatin does not catalyze nicotinamide mononucleotide formation in blood plasma. PLoS One 6, e22781.

Heer, C.D., Sanderson, D.J., Voth, L.S., Alhammad, Y.M.O., Schmidt, M.S., Trammell, S. A.J., Perlman, S., Cohen, M.S., Fehr, A.R., Brenner, C., 2020. Coronavirus infection and PARP expression dysregulate the NAD metabolome: an actionable component of innate immunity. J. Biol. Chem. 295, 17986–17996.

Hiefner, J., Rische, J., Bunders, M.J., Worthmann, A., 2023. A liquid chromatography-tandem mass spectrometry based method for the quantification of adenosine nucleotides and NAD precursors and products in various biological samples. Front. Immunol. 14, 1250762.

Hoffman-Goetz, L., Pedersen, B.K., 1994. Exercise and the immune system: a model of the stress response? Immunol. Today 15, 382–387.

Holay, N., Kennedy, B.E., Murphy, J.P., Konda, P., Giacomantonio, M., Brauer-Chapin, T., Paulo, J.A., Kumar, V., Kim, Y., Elaghil, M., Sisson, G., Clements, D., Richardson, C., Gygi, S.P., Gujar, S., 2023. After virus exposure, early bystander naïve CD8 T cell activation relies on NAD+ salvage metabolism. Front. Immunol. 13, 1047661.

Immune function and exercise, 2011. N. P. Walsh, M. Gleeson, R. J. Shephard, M. Gleeson, J. A. Woods, N. C. Bishop, M. Fleshner, C. Green, B. K. Pedersen, L. Hoffman-Goetz, C. J. Rogers, H. Northoff, A. Abbasi, P. Simon, Position statement. Part one. Exerc. Immunol. Rev. 17, 6–63.

Ito, Y., Yonekura, R., Nakagami, Y., Maruta, K., Koike, T., Nagamura, Y., Shibata, K., Saito, K., 2003. In: Allegri, G., Costa, C. V. L., Ragazzi, E., Steinhart, H., Varesio, L. (Eds.), Developments in Tryptophan and Serotonin Metabolism, Springer US, Boston, MA, pp. 531–535.

Izadpanah, A., Mudd, J.C., Garcia, J.G.N., Srivastav, S., Abdel-Mohsen, M., Palmer, C., Goldman, A.R., Kolls, J.K., Qin, X., Rappaport, J., 2023. SARS-CoV-2 infection dysregulates NAD metabolism. Front. Immunol. 14, 1158455.

Jae, S.Y., Heffernan, K.S., Kurl, S., Kunutsor, S.K., Kim, C.-H., Johnson, B.D., Franklin, B. A., Laukkanen, J.A., 2021. Cardiorespiratory Fitness, Inflammation, and the Incident Risk of Pneumonia. J. Cardiopulm. Rehabil. Prev. 41. https://journals.lww.com/jcrjournal/fulltext/2021/05000/cardiorespiratory_fitness,_inflammation,_and_the.12.aspx.

Janssen, H., Koekkoek, L.L., Swirski, F.K., 2023. Effects of lifestyle factors on leukocytes in cardiovascular health and disease. Nat Rev Cardiol. https://doi.org/10.1038/s41569-023-00931-w.

Joisten, N., Walzik, D., Schenk, A., Metcalfe, A.J., Belen, S., Schaaf, K., Jacko, D., Gehlert, S., Spiliopoulou, P., Garzinsky, A.-M., Thevis, M., Rappelt, L., Donath, L., Meuth, S.G., Bloch, W., Zimmer, P., 2024. Acute exercise activates the AHR in peripheral blood mononuclear cells in an intensity-dependent manner. Am. J. Phys. Cell Phys. 327, C438–C445.

Kaminsky, L.A., Arena, R., Myers, J., Peterman, J.E., Bonikowske, A.R., Harber, M.P., Medina Inojosa, J.R., Lavie, C.J., Squires, R.W., 2022. Updated reference standards for cardiorespiratory fitness measured with cardiopulmonary exercise testing. Mayo Clin. Proc. 97, 285–293.

Katsyuba, E., Romani, M., Hofer, D., Auwerx, J., 2020. NAD+ homeostasis in health and disease. Nature Metabolism 2, 9–31.

Klein, S.L., Flanagan, K.L., 2016. Sex differences in immune responses. Nat Rev Immunol 16, 626–638.

Kurz, E., Hirsch, C.A., Dalton, T., Shadaloey, S.A., Khodadadi-Jamayran, A., Miller, G., Pareek, S., Rajaei, H., Mohindroo, C., Baydogan, S., Ngo-Huang, A., Parker, N., Katz, M.H.G., Petzel, M., Vucic, E., McAllister, F., Schadler, K., Winograd, R., Bar-Sagi, D., 2022. Exercise-induced engagement of the IL-15/IL-15Rα axis promotes anti-tumor immunity in pancreatic cancer. Cancer Cell 40, 720–737.e5.

Liu, L., Su, X., Quinn, W.J., Hui, S., Krukenberg, K., Frederick, D.W., Redpath, P., Zhan, L., Chellappa, K., White, E., Migaud, M., Mitchison, T.J., Baur, J.A., Rabinowitz, J.D., 2018. Quantitative analysis of NAD synthesis-breakdown fluxes. Cell Metab. 27, 1067–1080.e5.

Martens, C.R., Denman, B.A., Mazzo, M.R., Armstrong, M.L., Reisdorph, N., McQueen, M. B., Chonchol, M., Seals, D.R., 2018. Chronic nicotinamide riboside supplementation is well-tolerated and elevates NAD+ in healthy middle-aged and older adults. Nat. Commun. 9, 1286.

Membrez, M., Migliavacca, E., Christen, S., Yaku, K., Trieu, J., Lee, A.K., Morandini, F., Giner, M.P., Stiner, J., Makarov, M.V., Garratt, E.S., Vasiloglou, M.F., Chanvillard, L., Dalbram, E., Ehrlich, A.M., Sanchez-Garcia, J.L., Canto, C., Karagounis, L.G., Treebak, J.T., Migaud, M.E., Heshmat, R., Razi, F., Karnani, N., Ostovar, A., Farzadfar, F., Tay, S.K.H., Sanders, M.J., Lillycrop, K.A., Godfrey, K.M., Nakagawa, T., Moco, S., Koopman, R., Lynch, G.S., Sorrentino, V., Feige, J.N., 2024. Trigonelline is an NAD+ precursor that improves muscle function during ageing and is reduced in human sarcopenia. Nat. Metab. https://doi.org/10.1038/s42255-024-00997-x.

Midttun, Ø., Hustad, S., Ueland, P.M., 2009. Quantitative profiling of biomarkers related to B-vitamin status, tryptophan metabolism and inflammation in human plasma by liquid chromatography/tandem mass spectrometry. Rapid Comm. Mass Spectrometry 23, 1371–1379.

Minhas, P.S., Liu, L., Moon, P.K., Joshi, A.U., Dove, C., Mhatre, S., Contrepois, K., Wang, Q., Lee, B.A., Coronado, M., Bernstein, D., Snyder, M.P., Migaud, M., Majeti, R., Mochly-Rosen, D., Rabinowitz, J.D., Andreasson, K.I., 2019. Macrophage de novo NAD+ synthesis specifies immune function in aging and inflammation. Nat. Immunol. 20, 50–63.

Moore, S.C., Lee, I.-M., Weiderpass, E., Campbell, P.T., Sampson, J.N., Kitahara, C.M., Keadle, S.K., Arem, H., Berrington De Gonzalez, A., Hartge, P., Adami, H.-O., Blair, C.K., Borch, K.B., Boyd, E., Check, D.P., Fournier, A., Freedman, N.D., Gunter, M., Johannson, M., Khaw, K.-T., Linet, M.S., Orsini, N., Park, Y., Riboli, E., Robien, K., Schairer, C., Sesso, H., Spriggs, M., Van Dusen, R., Wolk, A., Matthews, C.

E., Patel, A.V., 2016. Association of Leisure-Time Physical Activity With Risk of 26 Types of Cancer in 1.44 Million Adults. *JAMA*. Intern Med 176, 816.
Mouchiroud, L., Houtkooper, R.H., Auwerx, J., 2013. NAD $^{+}$ metabolism: a therapeutic target for age-related metabolic disease. Crit. Rev. Biochem. Mol. Biol. 48, 397–408.
Müller-Durovic, B., Jäger, J., Engelmann, C., Schuhmachers, P., Altermatt, S., Schlup, Y., Duthaler, U., Makowiec, C., Unterstab, G., Roffeis, S., Xhafa, E., Assmann, N., Trulsson, F., Steiner, R., Edwards-Hicks, J., West, J., Turner, L., Develioglu, L., Ivanek, R., Azzi, T., Dehio, P., Berger, C., Swiss Transplant Cohort Study#, Kuzmin, D., Saboz, S., Mautner, J., Löliger, J., Geigges, M., Palianina, D., Khanna, N., Dirnhofer, S., Münz, C., Bantug, G.R., Hess, C., Berger, C., Hess, C., Koller, M., Rossi, S., Stampf, S., Müller, N.J., 2024. A metabolic dependency of EBV can be targeted to hinder B cell transformation. Science.
Nakahata, Y., Sahar, S., Astarita, G., Kaluzova, M., Sassone-Corsi, P., 2009. Circadian Control of the NAD $^{+}$ Salvage Pathway by CLOCK-SIRT1. Science 324, 654–657.
Palzer, L., Bader, J.J., Angel, F., Witzel, M., Blaser, S., McNeil, A., Wandersee, M.K., Leu, N.A., Lengner, C.J., Cho, C.E., Welch, K.D., Kirkland, J.B., Meyer, R.G., Meyer-Ficca, M.L., 2018. Alpha-amino-beta-carboxy-muconate-semialdehyde decarboxylase controls dietary niacin requirements for NAD+ synthesis. Cell Rep. 25, 1359–1370.e4.
Pang, H., Jiang, Y., Li, J., Wang, Y., Nie, M., Xiao, N., Wang, S., Song, Z., Ji, F., Chang, Y., Zheng, Y., Yao, K., Yao, L., Li, S., Li, P., Song, L., Lan, X., Xu, Z., Hu, Z., 2021. Aberrant NAD+ metabolism underlies Zika virus–induced microcephaly. Nat. Metab. 3, 1109–1124.
Patel, A.V., Friedenreich, C.M., Moore, S.C., Hayes, S.C., Silver, J.K., Campbell, K.L., Winters-Stone, K., Gerber, L.H., George, S.M., Fulton, J.E., Denlinger, C., Morris, G. S., Hue, T., Schmitz, K.H., Matthews, C.E., 2019. American college of sports medicine roundtable report on physical activity, sedentary behavior, and cancer prevention and control. Med. Sci. Sports Exerc. 51, 2391–2402.
Pedersen, B.K., Hoffman-Goetz, L., 2000. Exercise and the immune system: regulation, integration, and adaptation. Physiol. Rev. 80, 1055–1081.
Pedersen, L., Idorn, M., Olofsson, G.H., Lauenborg, B., Nookaew, I., Hansen, R.H., Johannesen, H.H., Becker, J.C., Pedersen, K.S., Dethlefsen, C., Nielsen, J., Gehl, J., Pedersen, B.K., Thor Straten, P., Hojman, P., 2016. Voluntary running suppresses tumor growth through epinephrine- and IL-6-dependent NK cell mobilization and redistribution. Cell Metab. 23, 554–562.
Peluso, A., Damgaard, M.V., Mori, M.A.S., Treebak, J.T., 2021. Age-dependent decline of NAD+—universal truth or confounded consensus? Nutrients 14, 101.
Rajman, L., Chwalek, K., Sinclair, D.A., 2018. Therapeutic potential of NAD-boosting molecules: the in vivo evidence. Cell Metab. 27, 529–547.
Ramsey, K.M., Yoshino, J., Brace, C.S., Abrassart, D., Kobayashi, Y., Marcheva, B., Hong, H.-K., Chong, J.L., Buhr, E.D., Lee, C., Takahashi, J.S., Imai, S., Bass, J., 2009. Circadian clock feedback cycle through NAMPT-mediated NAD^{+} biosynthesis. Science 324, 651–654.
Remie, C.M., Roumans, K.H., Moonen, M.P., Connell, N.J., Havekes, B., Mevenkamp, J., Lindeboom, L., De Wit, V.H., Van De Weijer, T., Aarts, S.A., Lutgens, E., Schomakers, B.V., Elfrink, H.L., Zapata-Pérez, R., Houtkooper, R.H., Auwerx, J., Hoeks, J., Schrauwen-Hinderling, V.B., Phielix, E., Schrauwen, P., 2020. Nicotinamide riboside supplementation alters body composition and skeletal muscle acetylcarnitine concentrations in healthy obese humans. Am. J. Clin. Nutr. 112, 413–426.
Revollo, J.R., Grimm, A.A., Imai, S., 2004. The NAD biosynthesis pathway mediated by nicotinamide phosphoribosyltransferase regulates Sir2 activity in mammalian cells. J. Biol. Chem. 279, 50754–50763.
Rongvaux, A., Shea, R.J., Mulks, M.H., Gigot, D., Urbain, J., Leo, O., Andris, F., 2002. Pre-B-cell colony-enhancing factor, whose expression is up-regulated in activated lymphocytes, is a nicotinamide phosphoribosyltransferase, a cytosolic enzyme involved in NAD biosynthesis. Eur. J. Immunol. 32, 3225–3234.
Rumpf, C., Proschinger, S., Schenk, A., Bloch, W., Lampit, A., Javelle, F., Zimmer, P., 2021. The effect of acute physical exercise on NK-cell cytolytic activity: a systematic review and meta-analysis. Sports Med. 51, 519–530.
Rundqvist, H., Veliça, P., Barbieri, L., Gameiro, P.A., Bargiela, D., Gojkovic, M., Mijwel, S., Reitzner, S.M., Wulliman, D., Ahlstedt, E., Ule, J., Östman, A., Johnson, R.S., 2020. Cytotoxic T-cells mediate exercise-induced reductions in tumor growth. Elife 9, e59996.
Sato, T., Sassone-Corsi, P., 2022. Nutrition, metabolism, and epigenetics: pathways of circadian reprogramming. EMBO Rep. 23. https://doi.org/10.15252/embr.202152412.
Savikj, M., Stocks, B., Sato, S., Caidahl, K., Krook, A., Deshmukh, A.S., Zierath, J.R., Wallberg-Henriksson, H., 2022. Exercise timing influences multi-tissue metabolome and skeletal muscle proteome profiles in type 2 diabetic patients – a randomized crossover trial. Metabolism 135, 155268.
Schlagheck, M.L., Walzik, D., Joisten, N., Koliamitra, C., Hardt, L., Metcalfe, A.J., Wahl, P., Bloch, W., Schenk, A., Zimmer, P., 2020. Cellular immune response to acute exercise: Comparison of endurance and resistance exercise. Eur. J. Haematol. 105, 75–84.
Schwarcz, R., Bruno, J.P., Muchowski, P.J., Wu, H.-Q., 2012. Kynurenines in the mammalian brain: when physiology meets pathology. Nat. Rev. Neurosci. 13, 465–477.
Scott, N.W., McPherson, G.C., Ramsay, C.R., Campbell, M.K., 2002. The method of minimization for allocation to clinical trials. Control. Clin. Trials 23, 662–674.
Shi, C., Wen, Z., Yang, Y., Shi, L., Liu, D., 2024. NAD+ metabolism and therapeutic strategies in cardiovascular diseases. Atherosclerosis Plus 57, 1–12.
Trammell, S.A.J., Weidemann, B.J., Chadda, A., Yorek, M.S., Holmes, A., Coppey, L.J., Obrosov, A., Kardon, R.H., Yorek, M.A., Brenner, C., 2016. Nicotinamide riboside opposes type 2 diabetes and neuropathy in mice. Sci. Rep. 6, 26933.
Trammell, S.A.J., Schmidt, M.S., Weidemann, B.J., Redpath, P., Jaksch, F., Dellinger, R. W., Li, Z., Abel, E.D., Migaud, M.E., Brenner, C., 2016. Nicotinamide riboside is uniquely and orally bioavailable in mice and humans. Nat. Commun. 7, 12948.
Vaur, P., Brugg, B., Mericskay, M., Li, Z., Schmidt, M.S., Vivien, D., Orset, C., Jacotot, E., Brenner, C., Duplus, E., 2017. Nicotinamide riboside, a form of vitamin B3, protects against excitotoxicity-induced axonal degeneration. FASEB J. 31, 5440–5452.
Walzik, D., Jonas, W., Joisten, N., Belen, S., Wüst, R.C.I., Guillemin, G., Zimmer, P., 2023. Tissue-specific effects of exercise as NAD+-boosting strategy: Current knowledge and future perspectives. Acta Physiol. https://doi.org/10.1111/apha.13921.
Wan, J., Cheng, C., Hu, J., Huang, H., Han, Q., Jie, Z., Zou, Q., Shi, J.-H., Yu, X., 2023. De novo NAD+ synthesis contributes to CD8+ T cell metabolic fitness and antitumor function. Cell Rep. 42, 113518.
Wang, D.D., Airhart, S.E., Zhou, B., Shireman, L.M., Jiang, S., Melendez Rodriguez, C., Kirkpatrick, J.N., Shen, D.D., Tian, R., O'Brien, K.D., 2022. Safety and tolerability of nicotinamide riboside in heart failure with reduced ejection fraction. JACC: Basic Translational Sci. 7, 1183–1196.
Wang, Y., Wang, F., Wang, L., Qiu, S., Yao, Y., Yan, C., Xiong, X., Chen, X., Ji, Q., Cao, J., Gao, G., Li, D., Zhang, L., Guo, Z., Wang, R., Wang, H., Fan, G., 2021. NAD+ supplement potentiates tumor-killing function by rescuing defective TUB-mediated NAMPT transcription in tumor-infiltrated T cells. Cell Rep. 36, 109516.
Wu, J., Singh, K., Lin, A., Meadows, A.M., Wu, K., Shing, V., Bley, M., Hassanzadeh, S., Huffstutler, R.D., Schmidt, M.S., Blanco, L.P., Tian, R., Brenner, C., Pirooznia, M., Kaplan, M.J., Sack, M.N., 2022. Boosting NAD+ blunts TLR4-induced type I IFN in control and systemic lupus erythematosus monocytes. J. Clin. Investig. 132, e139828.
Yoshino, J., Baur, J.A., Imai, S., 2018. NAD+ intermediates: the biology and therapeutic potential of NMN and NR. Cell Metab. 27, 513–528.
Zapata-Pérez, R., Wanders, R.J.A., Karnebeek, C.D.M., Houtkooper, R.H., 2021. NAD $^{+}$ homeostasis in human health and disease. EMBO Mol Med 13. https://doi.org/10.15252/emmm.202113943.
Zheng, M., Schultz, M.B., Sinclair, D.A., 2022. NAD+ in COVID-19 and viral infections. Trends Immunol. 43, 283–295.
Zhou, B., Wang, D.-D.-H., Qiu, Y., Airhart, S., Liu, Y., Stempien-Otero, A., O'Brien, K.D., Tian, R., 2020. Boosting NAD level suppresses inflammatory activation of PBMCs in heart failure. J. Clin. Investig. 130, 6054–6063.